MICROSTRIP PHASED ARRAY ANTENNAS PRINTED ON INCLINED PLANES

Daniel AUGUSTIN, Robert STARAJ,
Edmond CAMBIAGGIO, Albert PAPIERNIK

Laboratoire d' Electronique
Université de Nice - Sophia Antipolis
Unité de Recherche Associée au CNRS n° 1400 - 250,
rue A. Einstein, 06 560 Valbonne, France
Tél. : 92.94.28.10 - Fax : 92.94.28.12

Abstract

This paper presents an analysis of the electromagnetic field radiated by microstrip patch antennas printed on inclined surfaces. The theoretical approach allows to apply spatial rotations to each source. The computer simulation developed permits us to experiment different antenna structures and two original realisations are proposed: a 2-element array printed on two inclined planes and a 4-element array laid out on a pyramidal surface. In addition, it enables the choice of the phase applied to each radiator to produce a beam deflection function. A good accuracy is obtained between theoretical and experimental results. The aim of this study is to optimise the parameters of such antennas to achieve the desired radiation patterns, from printed phased arrays on conformal surfaces. We also present the theoretical behaviour of a octagonal pyramid.

1. Introduction

The applications of microstrip antennas, printed on conformal surfaces, are various and many studies have been specially made for radio mobile communications, satellites, spacecrafts and aircrafts [1-7]. In fact, these studies are increasing due to the many advantages of the microstrip resonators as the little weight, the low cost, the electronic tracking, the easy integration of active devices, ect...To produce spatial tracking specifications, belt and ring array antennas, arranged on cylindrical sections, are generally used and many authors have treated this subject [2][4]. However, the computer-aided analysis of radiation patterns of structures made up of antennas arranged in the three dimensions of the space, is relatively difficult and not very developed in specialised literature. Moreover, some studies have considered the case of planar arrays made up of microstrip radiators with different directions of polarisation, mainly obtained by rotations of 90° or 180° [5] but the studies in conformal arrays generally consider the same direction of polarisation for all the elements.

So, our study has consisted in working out a theoretical approach and an algorithm to enable spatial rotations instead of planar ones and so, to configure this ring antenna on spherical, conical, pyramidal or cylindrical surfaces, as shown on figures 1 and 2, and this, with a direction of polarisation totally free. The first step of our research consisted in the study of microstrip antenna arrays with arbitrary planar rotations. This allowed us to analyse the radiation pattern of a phased ring antenna of 8 linearly polarised patches, to produce a very good circular polarisation in a very small angular aperture [6]. The second step has consisted in calculating the electric field resulting from different rotations in the space of a group of antennas.

In this article, we will present the theoretical and practical behavior of the radiation patterns of our two structures, composed by 2 and 4 elements, as shown on figures 3 and 4 and the theoretical study of an octogonal antenna (figure 5).

Figure 7 shows the notations used for this analysis in the case of the "two-slope" array : patches move by rotating an angle ρ about OX'-axis). The pyramidal and octagonal arrays (figure 4 and 5) represent a more complicated version, but keep the same notations with one more rotation by an angle Ψ_i about OZ'-axis.

2. Theoretical approach

The **stationary** coordinate system OX'Y'Z' is named **global (g)** coordinate system (figure 6). Another coordinate frame, called **local (l)** system is associated to the source in rotation in space. Figure 7 presents the basic two-slope array which consists in two linearly polarised radiators etched on a thin dielectric substrate. The objective is to analyse the far electric field in the g-system, taking into account the influence of all rotated and inclined sources. To reach this result, we determine the initial electric field, noted $E_i(\Theta,\Phi)$* and radiated by the S_i source in the l-system. The coordinates (Θ,Φ) are the spherical coordinates of the observation points, calculated from the spherical coordinates (Θ',Φ') in the g-system. S_1 , polarised along the OY' axis, was taken as the reference source (figure 7). The angular rotations ρ (around the OX' axis) and / or Ψ_i (around the OZ' axis) effects, are given by the Eulerian matrix $[P_i]$ for every radiating element S_i.

** The italic notation is used for field vectors*

The expression of the Eulerian matrix changes with the rotation choice, as follows :

♦ For the 0Z'-rotation and 0X'-rotation respectively, we have :

$$[P_i]=[P_{Z\,i}]=\begin{bmatrix} \cos\Psi_i & \sin\Psi_i & 0 \\ -\sin\Psi_i & \cos\Psi_i & 0 \\ 0 & 0 & 1 \end{bmatrix}$$

$$[P_i]=[P_X]=\begin{bmatrix} 1 & 0 & 0 \\ 0 & \cos\rho & \sin\rho \\ 0 & -\sin\rho & \cos\rho \end{bmatrix} \quad (1)$$

♦ For a 0X'-rotation followed by a 0Z'-rotation :

$$[P_i]=[P_{XZ\,i}]=\begin{bmatrix} \cos\Psi_i & \sin\Psi_i & 0 \\ -\sin\Psi_i.\cos\rho & \cos\Psi_i.\cos\rho & \sin\rho \\ \sin\Psi_i.\sin\rho & -\cos\Psi_i.\sin\rho & \cos\rho \end{bmatrix} \quad (2)$$

Then, the electrical far field radiated by the i^{th} element (initial field expressed by its components E_Θ and E_Φ) is calculated by a surface current method. The transition between the local coordinate system after rotation and the global coordinate system, where the final result will be obtained, is taken into account in the expression of this field. The final field $E_{fi}\ (\Theta',\Phi')^*$ for each source after the rotations, expressed in the g-system, is obtained by the product of the initial field with the result of a transformation matrices product. This one consists in the multiplication between one of the Eulerian matrix $[P_i]$ (depending on the rotation(s) applied) and the coordinate transformation matrices [M1] and [M2] defined as :

♦ For the l-system (spherical to rectangular transformation) :

$$[M1]=\begin{bmatrix} \sin\Theta.\cos\Phi & \cos\Theta.\cos\Phi & -\sin\Phi \\ \sin\Theta.\sin\Phi & \cos\Theta.\sin\Phi & \cos\Phi \\ \cos\Theta & -\sin\Theta & 0 \end{bmatrix} \quad (3)$$

♦ For the g-system (rectangular to spherical transformation) :

$$[M2]=\begin{bmatrix} \sin\Theta'.\cos\Phi' & \sin\Theta'.\sin\Phi' & \cos\Theta' \\ \cos\Theta'.\cos\Phi' & \cos\Theta'.\sin\Phi' & -\sin\Theta' \\ -\sin\Phi' & \cos\Phi' & 0 \end{bmatrix} \quad (4)$$

Concurrently, a term FR_i describes the influence of the position (spatial distribution : d-translation and φ_i-angular position), the phase α_i and the amplitude A_i of the exciting current of each element [7] with the expression as follows :

$$FR_i = A_i\, e^{j\,[(2\pi/\lambda)\,d\,(\cos\varphi_i\sin\theta'\cos\Phi' + \sin\varphi_i\sin\theta'\sin\Phi') + \alpha_i]} \quad (5)$$

For n elements, the **total field** is finally given, in g-system, by :

$$E_{tot}(\Theta',\Phi') = \sum_{i=1}^{n} E_{fi}\,(\Theta',\Phi')\ FR_i(\Theta',\Phi') \quad (6)$$

The advantages of this method, compared to other studies [3-4], is that you can quickly change the radiatiąting element and calculate very rapidly the new radiation pattern. You only need the radiation pattern, calculated or measured, of the single element you want to use.

3. Realisation and measurements

The square microstrip patches used are linearly polarised, and the work frequency is situated in the C-band. All the identical radiators are probe-fed and their dimensions and feed positions are optimised to obtain a matched input impedance at the resonant frequency of 5 GHz.
The studied arrays are as follows :

♦ **Two-slope array** : The sources (S1, S2) with the same phase (figure 3) rotate respectively by angles (-ρ,ρ) about OX'-axis and are translated from the O-reference point of **g**, at **d** position. The realisation allows to modify the ρ-angle. Consequently, **d** also changes and we can make a parameter study : directivity behavior of the antenna.

♦ **Pyramidal array** : Each S_i source rotates by an angle Ψ_i about OZ'-axis (figure 4). Then, we apply another rotation by an angle ρ about OX'-axis and a translation **d** from the O-reference point of **g**. Here, the practical realisation of this array has been fixed with ρ = 30° and d= 3.42 cm. The phases of patches are either the same, or 0° for S_1 and S_2 and 180° for S_3 and S_4.

♦ **Octagonal array** : Each S_i source rotates by an angle Ψ_i about OZ'-axis.(figure 5). Then, we apply another rotation by an angle ρ about OX'-axis and a translation **d** from the O-reference point of **g**. Only the theoretical study is done for this array and a linear or a circular polarisation can be investigated.

Each patch is fed by a metallic pin through the dielectric substrate and the ground plane. Two power dividers have been realised with microstrip technology to obtain the desired amplitude and phase shift. The lengths of the different feed lines have been optimised by CAD and we can conclude that the coupling effects are considerably reduced considering the distance between the patches and the conformal disposition. The measurements of the input impedance are quite good.

The comparison between computed and measured electric field is given figures 8 to 13 for different configurations and current phases of the two-slope and pyramidal array. This kind of representation allows to know exactly the value of the electrical far-field radiated in each direction of the space. However, in most of the applications like telemetry, telecommand, teledetection, telecommunication or control using this type of 3-D structures, the requirement is generally an omnidirectionnal field or a constant value for an angle θ from the z-axis. For this reason, a 3-D representaion of the field is more interesting to see quickly the properties of the antenna. Two calculated 3D-radiation patterns are presented (figures 14 and 15) to show the rotation effects on the electrical field and the directivity behavior. Figure 14 shows in 3-D representation the electric field represented figure 9.

Other type of representation are interesting too. For example, figure 16 presents the theoretical evolution of the electric field-component in the circumferential plane versus the variations of the observation-point angle. For the normal direction, the diagram represents the circular polarisation and when the observed point changes, we can see the degradation of the component. Figure 17 represents an original view of this circular polarisation for each direction (Θ',Φ'). The ellipticity of the polarisation is described by lozenges. These lozenges are a simulation of the ellipses representing the electrical magnitude field in rotation. The diagonals of these lozenges represent the axis of ellipses. We can see more easily where a linear or a circular polarisation is obtained.

4. Theoretical investigation

The problem is here to compare the radiated field of the three different structures of the figures 3, 4, and 5. The 3D representation is here chosen.

Figures 18 to 21 present the evolution of the radiation pattern since the planar ring array of various radius, until the pyramidal and octogonal one, in the case of a circular polarisation. We can easily see on these figures, the interest of a greater number of elements.

Figure 22 gives the theoretical behavior of the radiation pattern in the E-plane versus the slope-angle for the pyramidal antenna when the patches are linearly fed. Figure 23 shows this behavior for the octagonal body for two values of the slope-angle ρ.

5. Conclusion and prospects

The conformal antennas are used increasingly for communications between land and/or spatial mobiles. Their main advantages, in comparison with a planar solution, are their electronical and geometrical capabilities for a spatial tracking motion and the possibility to print

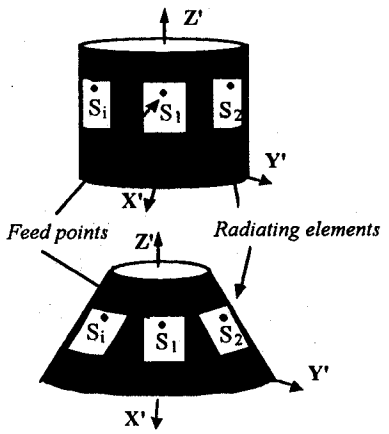

Fig.1 Conformal antennas printed on cylindrical and conical surfaces

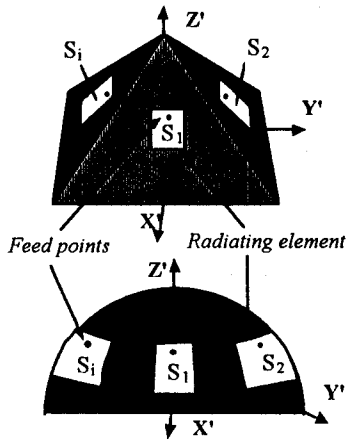

Fig.2 Conformal antennas printed on pyramidal and spherical surfaces

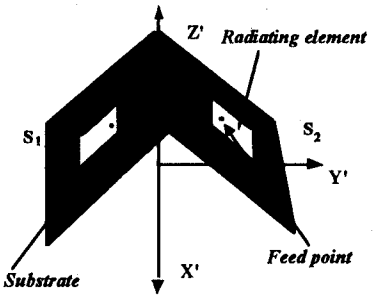

Fig.3 Two-slope array

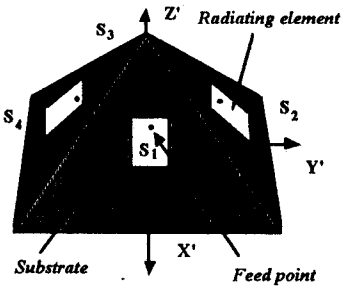

Fig. 4 Pyramidal array

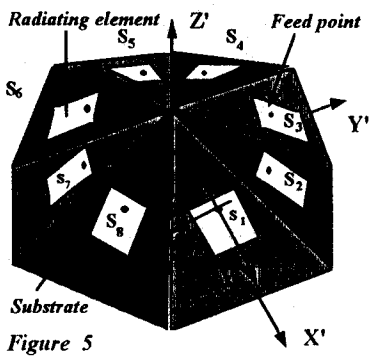

Fig. 5 Octagonal array

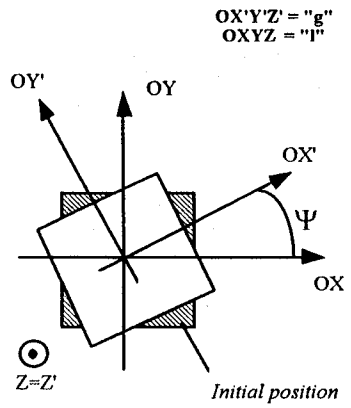

Fig. 6 Global "g" and local "l" coordinate systems

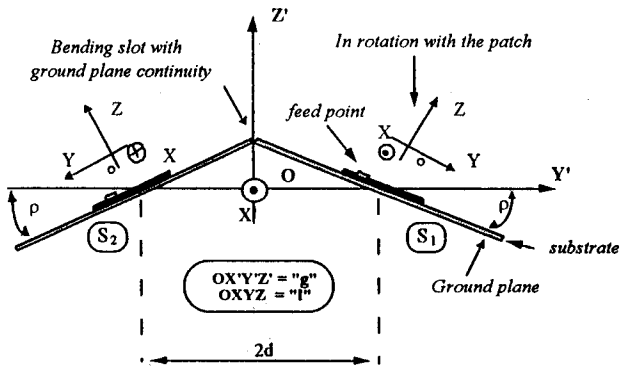

Fig. 7 "Double-slope" array with only one rotation of patches by angles about OX'-axis

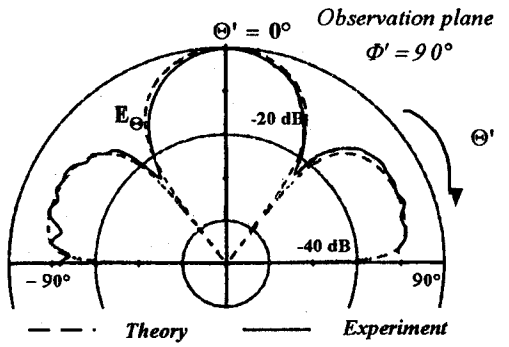

Fig. 8 E_θ component for the planar solution (ρ = 0°). Distance between the centres of the patches: 0.83 λ_0

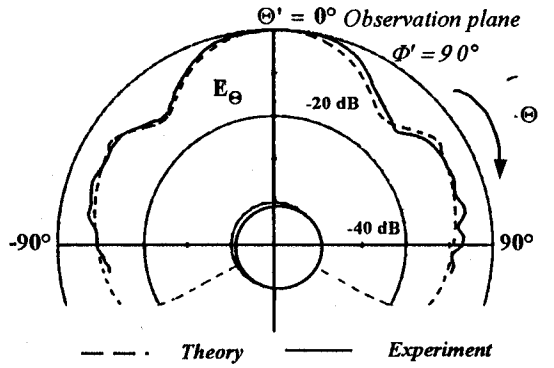

Fig. 9 E_θ component for ρ = 30° . Distance between the centres of the patches : 0.72 λ_0

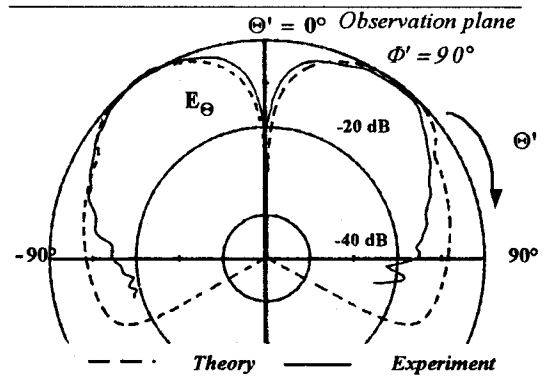

Fig. 10 Pyramidal array: Power divider assigns the same phase at each patch

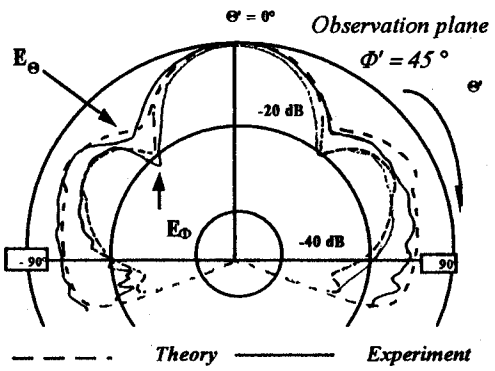

Fig. 11 Pyramidal array: Power divider assigns a sequential phase

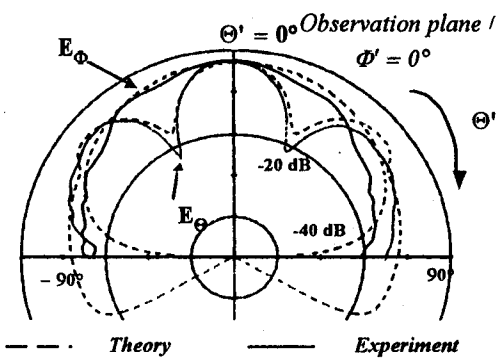

Fig. 12 Pyramidal array: The power divider assigns the phase 0° at S1 and S2 and 180° at S3 and S4

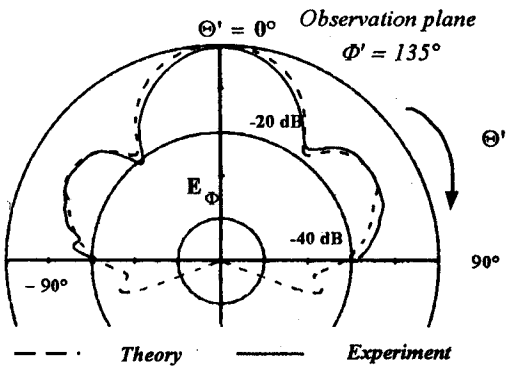

Fig. 13 Pyramidal array: The power divider assigns the phase 0° at S1 and S2 and 180° at S3 and S4

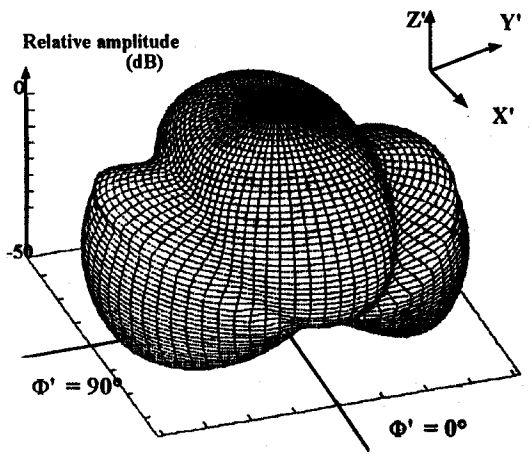

Fig. 14 3D-radiation pattern for the two-slope array with 30°-slope

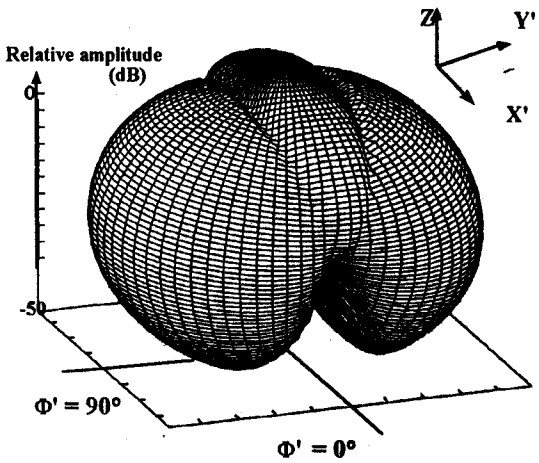

Fig. 15 3D-radiation pattern for the two-slope array with 70°-slope

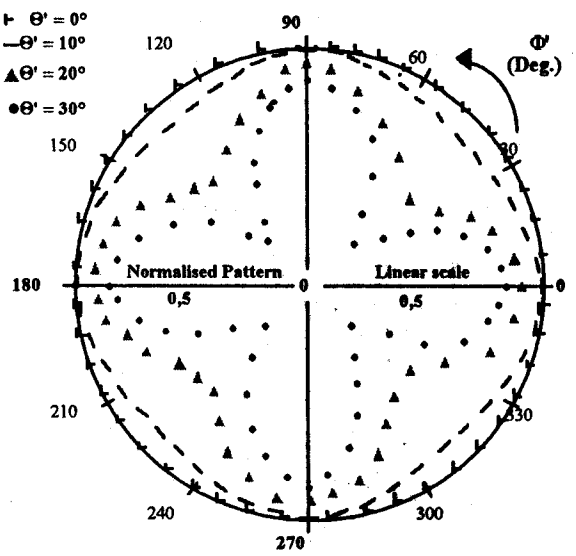

Fig. 16 Evolution of E_Φ in the circumferential plane of the pyramidal array

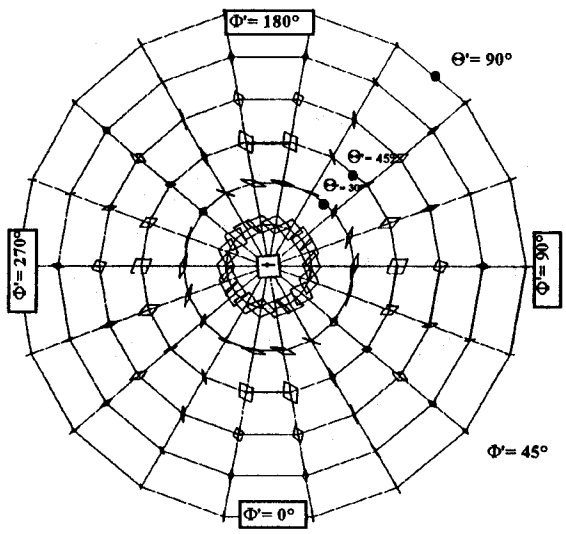

Fig. 17 Original view of the polarisation-rectangles for the pyramidal array

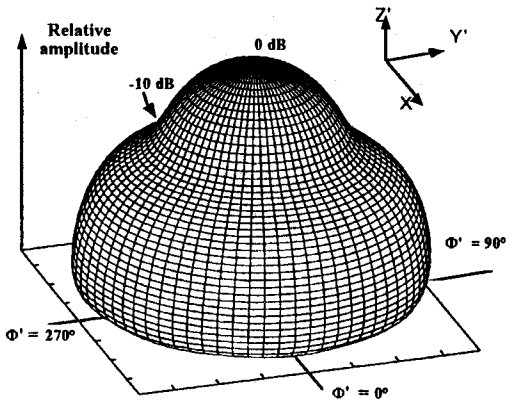

Fig. 18 3D-electrical field radiation pattern of the planar ring array

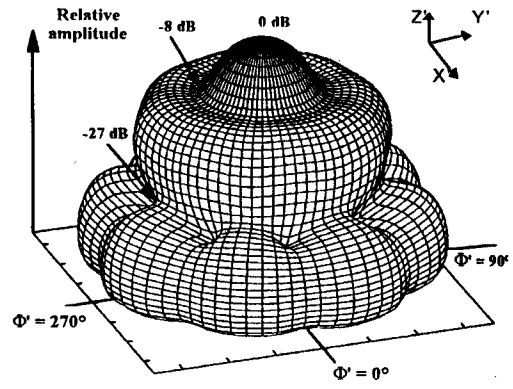

Fig. 19 3D-electrical field radiation pattern for a planar ring array with a higher radius

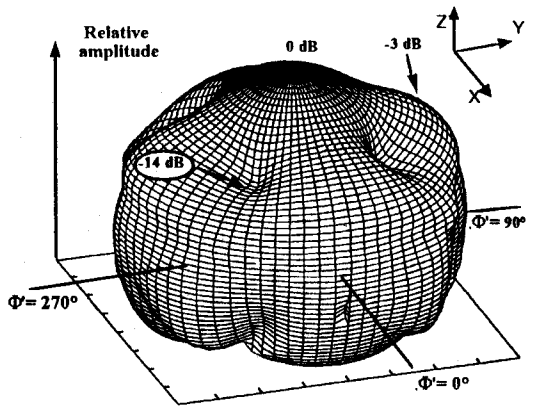

Fig. 20 3D-electrical field radiation pattern of the pyramidal array

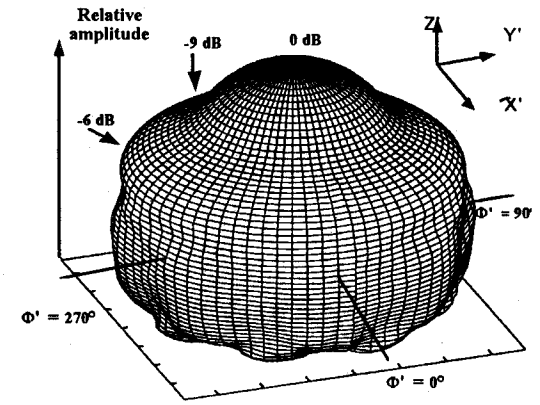

Fig. 21 3D-electrical field radiation pattern of the octagonal array

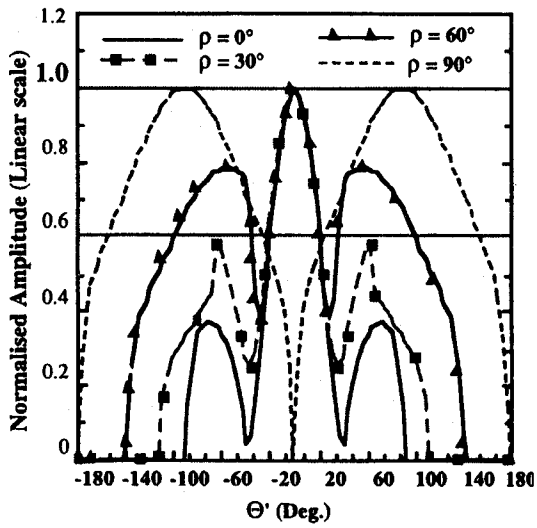

Fig. 22 Evolution of Eθ in the E-plane for the pyramidal array versus the variations of the ρ-slope

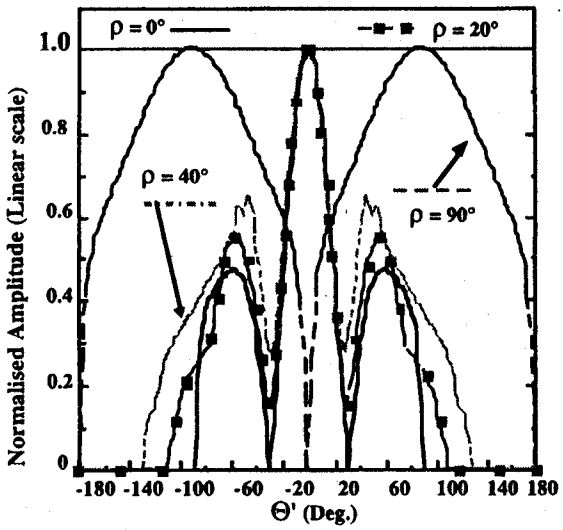

Fig. 23 Evolution of Eθ in the 45°-plane for the octagonal array versus the slope of the configuration

them on curved bodies. Our algorithm will enable, during the last stage, to arrange an array of radiating elements where we want in space, thanks to the control of the 3 basic rotations. The analysis approach of the conical structure will also enable to treat the cylindrical configuration for the particular case where ρ=90°. Moreover, it is planned to study a multi-ring array antenna system arranged on the same surface and thus to increase performance. The radiation patterns provided are in concordance with practical results. For a synthesis perspective, we will be able to optimise some parameters such as the distance d between centres of the patches, the rotation angles applied at each source, the number of active radiating elements and the phase shift associated to obtain a beam deflection function. For example, this study aims at providing a ripple ratio of the radiation patterns between [0,-10] dB for the relative amplitude, in the total space and close to a defined theoretical model. We will be able to evaluate the number of radiators to produce an efficient omnidirectional coverage. It is possible to improve the directivity performance of these antennas, thanks to the choice of the phase shift applied and the slope of the surface considered. Another prospect is to enable users of our algorithm to choose the shape of elements to be reduced, for example the dimensions of the global antenna.

References

[1] SCHRANK; "Basic theoretical aspects of spherical phased arrays"; Proceedings of the 1970 phased array antenna symposium; Phased array antennas, Oliner, Knittel, Artech house, Inc.; pp. 323-327.

[2] ASHKENZY, SHTRIKMAN, TREVES; "Electric surface current model for the analysis of microstrip antennas on cylindrical bodies"; 1985; IEEE TAP; Vol. AP 33, N°3; pp. 295-300.

[3] AUDOUY, DIEZ, RENAUD; "Synthesis of conformal array antennas"; 3rd Internationnal Conference on Electromagnetics in Aerospace Applications ICEAA'93; pp. 347-350, Torino, Italy, Sept. 93

[4] ROSTAN, GOTTWALD, WIESBECK; "Design and performance of conformal microstrip patch arrays o,n cylindrical surfaces"; 24th European Microwave Conference EuMC'94; Vol. 2; pp. 1756-1761, Cannes, France, Sept. 94

[5] HUANG; "A technique for an array to generate circular polarization with linearly polarized elements"; 1986; IEEE TAP; Vol. AP 34, N°9; pp. 1113-1124.

[6] AUGUSTIN, STARAJ, CAMBIAGGIO, PAPIERNIK; "Obtention de la polarisation circulaire par une antenne-réseau couronne"; 1993; 8eme JNM a Brest ; pp. 3D20-3D21.

[7] BALANIS; "Antenna theory, analysis and design"; 1982; Harper and Row Publishers, Inc.; pp. 275-282.

RADIOENGINEERING REVIEWERS

June 1996, Volume 5, Number 2

- P. Hudec, Czech Technical University, Prague
- M. Mazánek, Czech Technical University, Prague
- P. Martinek, Czech Technical University, Prague
- D. Černohorský, Technical University, Brno
- T. Dostál, Technical University, Brno
- J. Valsa, Technical University, Brno
- Z. Raida, Technical University, Brno
- Z. Smékal, Technical University, Košice
- J. Havlík, Military Academy, Brno